The Astronomical Journal, 154:79 (12pp), 2017 August https://doi.org/10.3847/1538-3881/aa7d50

Apparent Trend of the Iron Abundance in NGC 3201: The Same Outcome with Different Data

Valery V. Kravtsov[1,2]
[1] Departamento de Física, Facultad de Ciencias Naturales, Universidad de Atacama, Copayapu 485, Copiapó, Chile; valery.kravtsov@uda.cl
[2] Sternberg Astronomical Institute, Lomonosov Moscow State University, University Avenue 13, 119899 Moscow, Russia
Received 2016 April 26; revised 2017 June 26; accepted 2017 June 30; published 2017 August 1

Abstract

We further study the unusual trend we found at statistically significant levels in some globular clusters, including NGC 3201: a decreasing iron abundance in red giants toward the cluster centers. We first show that recently published new estimates of iron abundance in the cluster reproduce this trend, in spite of the authors' statement about no metallicity spread due to a low scatter achieved in the [Fe II/H] ratio. The mean of [Fe II/H] within $R \sim 2'$ from the cluster center is lower, by Δ[Fe II/H] $= 0.05 \pm 0.02$ dex, than in the outer region, in agreement with our original estimate for a much larger sample size within $R \approx 9'$. We found that an older data set traces the trend to a much larger radial distance, comparable with the cluster tidal radius, at Δ[Fe/H] ~ 0.2 dex, due to higher metallicity of distant stars. We conclude the trend is reproduced by independent data sets and find that it is accompanied by both a notable same-sign trend of oxygen abundance that can vary by up to Δ[O/Fe] ~ 0.3 dex within $R \approx 9'$ and an opposite-sign trend of sodium abundance.

Key words: globular clusters: general

1. Introduction

Analyzing archival data of elemental abundances in red giants (RGs) of a sample of so-called monometallic globular clusters (GCs), we found (Kravtsov 2013) a radial trend of iron abundance, statistically significant at high and very high confidence levels, in a number of the sample GCs. This trend is fairly unusual given (1) the fact of its existence in the GCs and (2) that the [Fe/H] ratio is lower, by about Δ[Fe/H] $\sim$ 0.05 dex, in the central than in the outer parts of the GCs. The key points to understand are (1) whether the trend is reproduced in independently obtained data sets on iron abundance in the same GCs, and, if this is the case, (2) whether it is caused by the real radial variation of iron abundance or by any kind of radial systematic effect mimicking it. The first point implies a need to study various data originating from observations gathered from different facilities and/or reduced independently.

In our original work (Kravtsov 2013), we used fairly uniform data on spectroscopy of large samples of RGs in a diversity of GCs (not less than 100 stars in each member of the GC sample: NGC 104, NGC 288, NGC 1851, NGC 3201, NGC 4590, NGC 5904, NGC 6121, NGC 6254, MGC 6752, and NGC 6809), obtained by Carretta et al. (2007, 2009, 2011) using the same facility, namely, the Very Large Telescope (VLT) FLAMES-GIRAFFE spectrograph ($R = 22{,}500$). For a sample of RGs in each GC, we compared the radial distributions (RDs) of stars with iron abundance higher (HIA) and lower (LIA) than the mean sample value as a diagnostic of a radial trend or segregation. The radial segregation between the subsamples of LIA and HIA RGs, in the sense of the former stars being more concentrated toward the centers of their parent GCs, was found using a Kolmogorov–Smirnov (K-S) test to be fairly high ($P = 92\%$) in NGC 6809 (M55) and statistically significant in 47 Tuc, NGC 1851, NGC 3201, and NGC 6752. Interestingly, three of the four latter GCs are highly concentrated, with central concentration $c > 2.00$ (Kravtsov 2013).

As for NGC 3201, Simmerer et al. (2013) determined the iron abundance for a sample of 25 of its RGs (using 21 previously obtained archival FLAMES-UVES spectra ($R \sim 40{,}000$) and 5 of their Magellan Inamori Kyocera Echelle (MIKE) spectra ($R \sim 40{,}000$)) and confirmed a spread in iron content found previously by Gonzalez & Wallerstein (1998). According to our estimate (Kravtsov 2013), the difference between the RDs of the LIA and HIA RGs of this sample turned out to be at a marginally statistically significant confidence level of $P = 96\%$, despite a fairly limited sample size. Note that the spectra used by Simmerer et al. (2013) are of higher resolution—approximately twice as much—than those used by Carretta et al. (2009).

Later, Mucciarelli et al. (2015) reanalyzed the same FLAMES-UVES spectra and came to a different conclusion about iron abundance spread in the GC. They found that while their estimates of the [Fe I/H] ratio are very similar to those published by Simmerer et al. (2013), the intrinsic spread of iron abundance derived from Fe II lines, in contrast, turned out to be much smaller. The authors explained that the larger dispersion in iron abundance estimates made by Simmerer et al. (2013) was due to a spurious effect, originating from unaccounted Non Local Thermodynamic Equilibrium (NLTE) effects in the analysis of possible Asymptotic Giant Branch (AGB) stars misidentified as Red Giant Branch (RGB) stars. Mucciarelli et al. (2015) concluded that NGC 3201 is a monometallic cluster with no evidence of iron spread.

Mucciarelli et al. (2015)'s conclusion is in disagreement with the results of Gonzalez & Wallerstein (1998), who determined elemental abundances in 18 RGs (using spectra with R varying between 13,500 and 42,000) and estimated reddening for the stars. Gonzalez & Wallerstein (1998) found an iron abundance range of Δ[Fe/H] $\sim$ 0.4–0.5 dex, 4 or 5 times as large as the uncertainties in iron abundance derived for an individual RG. They argued that this spread could not be attributed to the reddening variation and speculated that it could be caused by some kind of systematic effect "resulting from an unmodeled phenomenon in the atmospheres of cool giants, such as chromospheric heating and back-warming...." We refer the reader to that paper for more analysis of possible systematic

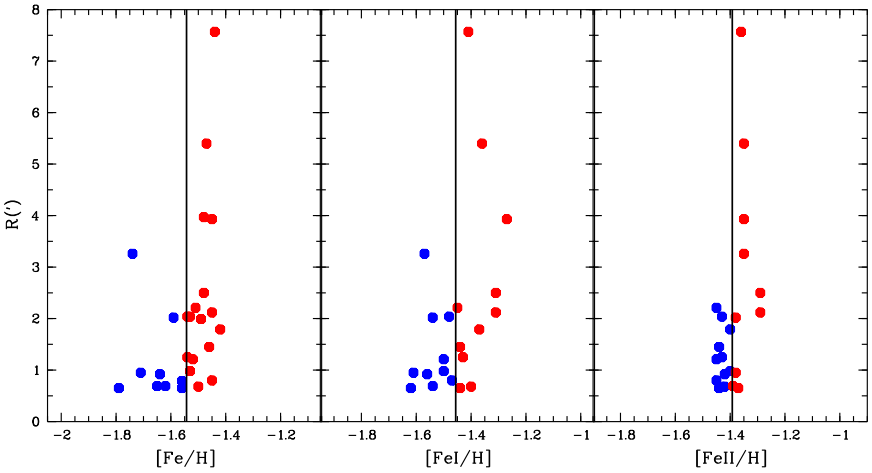

Figure 1. Dependence of iron abundance in RGs on their radial distance from the center of NGC 3201, based on the data obtained by Simmerer et al. (2013) from FLAMES-UVES (21 stars) and MIKE (5 stars) spectra (left panel) and by Mucciarelli et al. (2015) from Fe I and Fe II lines (middle and right panels, respectively) in the same FLAMES-UVES spectra. The vertical lines mark the mean values of [Fe/H].

effects. The Gonzalez & Wallerstein (1998) sample of RGs extends over a much larger radial distance from the cluster center, closely approaching the cluster's tidal limit of 28.′45 (Harris 1996). Then, the range in [Fe/H] found by Gonzalez & Wallerstein (1998) becomes more intriguing if it is related to how the [Fe/H] ratio depends on the radial distance from the cluster center (see discussion in Sections 3 and 4). By contrast, Muñoz et al. (2013), using high-resolution spectroscopy, found a significantly smaller dispersion of the [Fe/H] ratios derived for a sample of eight RGs within Δ[Fe/H] $\sim$ 0.12 dex that could be attributed to a real iron spread. However, their sample size is much smaller than those of Gonzalez & Wallerstein (1998), Simmerer et al. (2013), and Carretta et al. (2009). The furthest radial distance from the cluster center reached by the sample stars in Muñoz et al. (2013) is about 3.6 times as short as the cluster's tidal radius, but it is comparable to those reached by other data, except for the data of Gonzalez & Wallerstein (1998). The radial extent of each spectroscopic survey analyzed in the present paper can be seen in Figures 1 and 2.

In light of the result achieved by Mucciarelli et al. (2015), we first study whether their improved estimates of iron abundance in NGC 3201 are free of the radial trend appropriate to other data sets. Additionally, we include the Gonzalez & Wallerstein (1998) data in analyzing the dependence of iron abundance on projected radial distances (PRAD) from the cluster center. In addition to the radial trend (of the [Fe/H] ratio) under study, we show the presence of a notable same-sign radial trend of oxygen abundance. Finally, we discuss various effects that could mimic the radial [Fe/H] trend observed in RGs.

2. Data Analysis

The recently published archival data on iron abundance for 21 RGs in the GC NGC 3201, obtained by relying on both Fe I and Fe II lines in high-resolution FLAMES-UVES spectra and published by Mucciarelli et al. (2015), were taken from Table 1 of the paper. We refer to this paper for more details about the spectra used, data reduction and analysis, and the main conclusions reached. Moreover, for the purpose of comparison, we used the data of Gonzalez & Wallerstein (1998) (their Table 5), Carretta et al. (2009), and Simmerer et al. (2013)

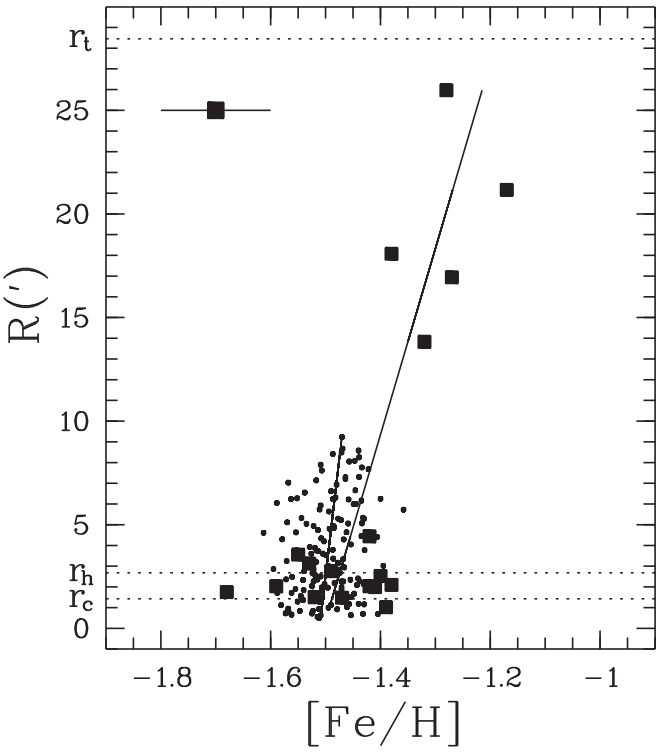

Figure 2. Comparison of the dependence of iron abundance in RGs on their radial distance from the center of NGC 3201, inferred from the data of Carretta et al. (2009) (149 stars; circles) and Gonzalez & Wallerstein (1998) (18 stars; squares). The solid lines are linear fits to the data. The error bar in the upper left corner of the figure shows the probable error estimated by Gonzalez & Wallerstein (1998) for the iron abundances they derived for separate stars. The dotted horizontal lines mark the core, half-mass, and tidal radii (r_c, r_h, and r_t, respectively) of NGC 3201.

(their Table 1). From the data of Mucciarelli et al. (2015) on the iron abundance of individual sample stars, we first calculated the mean values of the [Fe/H] ([Fe I/H] or [Fe II/H], depending on the data used) ratio. Then, as in Kravtsov (2013), we divided the total sample of RGs, $N_{\rm tot}$, into two subsamples of RGs with iron abundance lower ($N_{\rm LIA}$) and higher ($N_{\rm HIA}$) than its mean value, which were referred to as LIA and HIA RGs, respectively. For the RGs of the sample, we calculated their rectangular coordinates X ($\Delta\alpha''$), Y ($\Delta\delta''$), and PRAD ($R = \sqrt{X^2 + Y^2}$),

expressed in arcseconds, relative to the cluster center using the equatorial coordinates of the stars taken from Table 1 of Mucciarelli et al. (2015). In turn, the coordinates of the cluster center were taken from Harris (1996). Alternatively, the PRADs plotted in Figure 1 and expressed in arcminutes were taken from Simmerer et al. (2013). Finally, the probability (expressed in percent) P that the two subsamples had been drawn from different RDs in NGC 3201 was estimated by applying a K-S test.

Gonzalez & Wallerstein (1998) identified their sample stars with those from the list of Côté et al. (1994). We took the values of the PRADs of the respective stars from this list and used them in our analysis of the data of Gonzalez & Wallerstein (1998).

3. Results

In the three panels of Figure 1, we plot and compare the RDs of iron abundance in the GC NGC 3201 as inferred from the following sets of data: Simmerer et al. (2013) in the left panel followed by data from Mucciarelli et al. (2015) for the [Fe I/H] and [Fe II/H] ratio (middle and right panels, respectively). As we noted above, 21 stars are in common in both studies. The same plot for the data of Carretta et al. (2009) can be found in Kravtsov (2013) and in Figure 1 of the present paper. We show that the dispersion of points around the mean values of [Fe/H] (vertical lines) is comparable in the left and middle panels, while it is indeed notably smaller in the right panel showing the RD of the [Fe II/H] ratio. However, the most important point for our study is to compare the RDs of LIA and HIA RGs for the new data on iron abundance. For both [Fe I/H] and [Fe II/H] arrays of the estimates, the LIA RGs again turned out to be notably more centrally concentrated in the GC NGC 3201 than their HIA counterparts. Quantitative estimates, using a K-S test, support the apparent difference: despite a fairly limited total sample size of 21 stars, the RDs of the two subsamples of the RGs are different at a high confidence level of 92%. Moreover, in Figure 3, we show the positions and respective cumulative RDs of the LIA and HIA RGs of the sample in the field of NGC 3201 and compare them with the same plots for the data of Carretta et al. (2009). From this comparison, one can see that the difference between the cumulative RDs of LIA and HIA RGs in the data of Mucciarelli et al. 2015 is formally even larger than that in the data of Carretta et al. 2009 However, the sample size of the former data is unfortunately significantly smaller, which has resulted in a lower confidence level.

For the least dispersed [Fe II/H] ratio, we estimate the difference and its uncertainty between the mean iron abundance in the central and outer parts of the cluster. By drawing a boundary between the two parts around the PRAD of $R = 2'$, we find that the difference is close to Δ[Fe II/H] $= 0.05 \pm 0.02$ dex. In particular, Δ[Fe II/H] $= 0.054 \pm 0.022$ and Δ[Fe II/H] $= 0.052 \pm 0.020$ dex for the boundary drawn at exactly $R = 120''$ and $R = 107''$, respectively. It is evident that this is a very approximate estimate of both Δ[Fe II/H] and R, due to the limited sample size. The uncertainty is the standard error of the difference between the means of the two subsamples, and it has been calculated from the errors of the mean $(\sigma_i/\sqrt{N_i - 1})$ of each subsample. In addition to the notable difference in the RDs between the subsamples of LIA and HIA RGs in NGC 3201, the trend is also expressed in other quantitative form: the mean iron abundance in the central part of the cluster is lower, by 0.05 dex, than in the outer part, and it is 2.5 times as much as its error. The estimated Δ[Fe II/H] is formally indistinguishable, within the error, from our estimate of the magnitude of the trend (shown in Figure 2) that was originally made by relying on [Fe I/H] ratios derived by Carretta et al. (2009) for a much larger number of cluster RGs. We note that the standard deviations in both data sets, those obtained by Mucciarelli et al. (2015) and Carretta et al. (2009), are indistinguishable from each other and equal to $\sigma = 0.05$ dex. The error of the mean, however, is 2.6 times smaller in the latter data set, since the sample size is 7 times as large as the sample size of the former data set. Thus, acknowledging that the fact that the number of Fe II spectral lines is fewer than the number of Fe I lines in RG spectra, the final scatter (expressed in standard deviation of iron abundance estimates) reported by Mucciarelli et al. (2015, using Fe II lines) is not smaller than the scatter of the data derived by Carretta et al. (2009) by relying on Fe I lines.

The data of Carretta et al. (2009) are plotted, in the R versus [Fe/H] diagram, with circles in Figure 2 and overplotted with a continuous line that is a linear fit to these. The same is shown for the data on the iron abundance derived by Gonzalez & Wallerstein (1998) for their sample of 18 RGs. This figure shows that (1) the results on iron abundance obtained in both studies for stars falling in the same range of PRAD (i.e., at $R < 5'$) from the cluster center are in very good agreement within the uncertainty, but (2) the data of Gonzalez & Wallerstein (1998) reveal a much more pronounced radial trend of iron abundance, since the outermost five RGs (located at PRAD $R > 13'$) have, on average, obviously higher [Fe/H] ratios than the rest of the stars, 13 RGs, located within $R \approx 5'$. It is the essential difference in iron abundance between these two groups of stars that increased the range spanned by the [Fe/H] ratio derived by Gonzalez & Wallerstein (1998). The scatter in each group, in isolation from one another, is obviously lower than in the total sample. Indeed, the [Fe/H] ratio in the outermost stars varies in the range of $-1.38 \leqslant$ [Fe/H] $\leqslant -1.17$ dex, whereas the ratio in the inner RGs varies in the range of $-1.68 \leqslant$ [Fe/H] $\leqslant -1.38$ dex. The mean values of [Fe/H] and standard errors of the means for the outer and inner groups are $[\mathrm{Fe/H}]_{\mathrm{out}} = -1.28 \pm 0.04$ ($\sigma = 0.08$; five stars) and $[\mathrm{Fe/H}]_{\mathrm{inn}} = -1.48 \pm 0.03$ ($\sigma = 0.09$; 13 stars) dex, respectively. Hence, the difference between the means and its uncertainty are Δ[Fe/H] $= 0.20 \pm 0.05$ dex, in case of no systematic error. Therefore, the value of Δ[Fe/H] is 4 times as large as its formal random error that is the standard error of the difference between the means of the two subsamples. However, as was noted above, Gonzalez & Wallerstein (1998) supposed that the metallicities they derived may be affected by a systematic error. It is implied by the probable dependence of the estimated iron abundances in the sample RGs on the temperature of the stars. It is easy to see that the outer RGs have, on average, higher temperatures. So, the metallicity of the five outer RGs may really be lower, and, therefore, the magnitude of the radial trend may be smaller than 0.2 dex. It is apparently supported by the result of Covey et al. (2003), who reinvestigated the metallicity spread in NGC 3201 reported by Gonzalez & Wallerstein (1998). For the purpose of their study, Covey et al. (2003) gathered new spectra for six of the 18 RGs studied by Gonzalez & Wallerstein (1998). The rederived iron abundances for these six RGs, using spectroscopic temperatures, resulted in somewhat smaller metallicity differences between the most and least metal-rich stars (Côté 8 and Côté 246, respectively, from the list of Gonzalez & Wallerstein

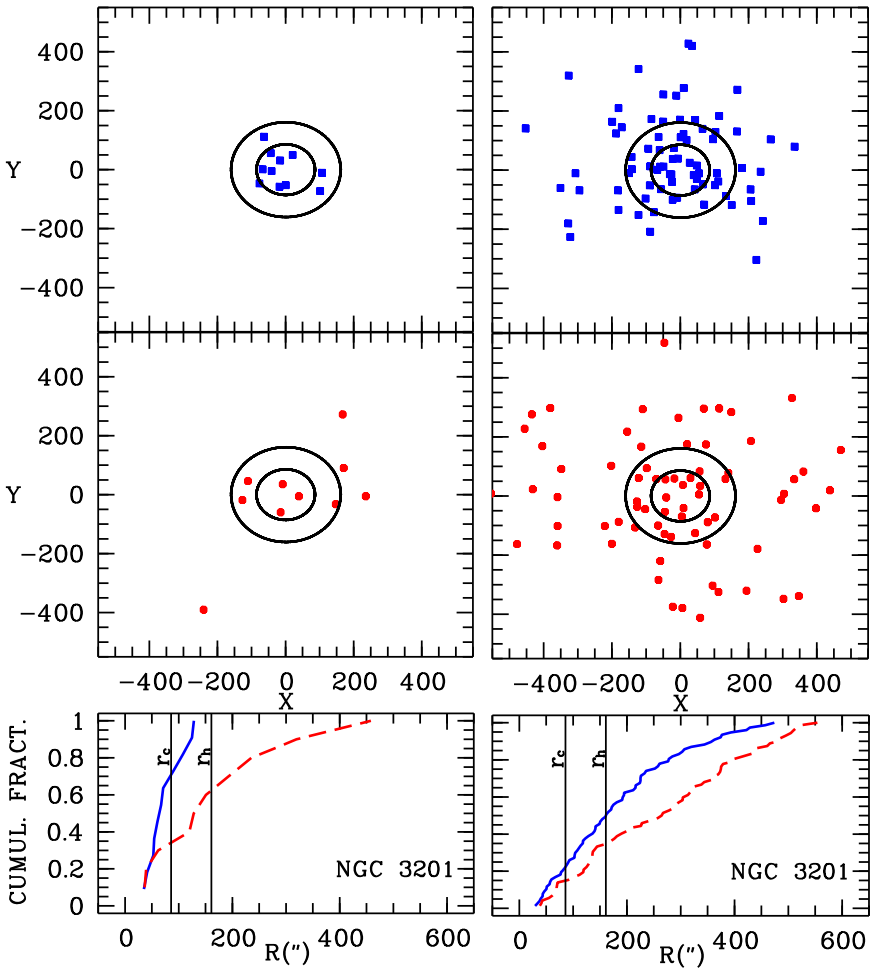

Figure 3. The positions (dots) and cumulative RDs (lines) of LIA (solid blue) and HIA (dashed red) RGs in the field of NGC 3201 are compared for the data of Mucciarelli et al. (2015) and Carretta et al. (2009) in the left and right columns, respectively. Both the *X, Y* coordinates and the PRAD, *R*, are in arcseconds. The smaller and larger circles show the cluster regions with the core and half-mass radii, respectively, of NGC 3201.

1998) but at the same mean error as compared to the results of Gonzalez & Wallerstein (1998). It should be noted, however, that Côté 8 is the only one of the five most metal-rich and most distant RGs in the sample of Gonzalez & Wallerstein (1998). Moreover, Côté 8 was not used to rederive iron abundance by relying alternatively on photometric temperatures. Overall, Covey et al. (2003) found an intriguing offset between metallicities they derived from photometrically and spectroscopically determined parameters.

The Covey et al. (2003) study could not quantify the difference in iron abundance between the outer RG population and those that are more centrally concentrated. Our present analysis shows, therefore, that a reliable answer to this question would have important implications for the formation and evolution of the cluster stellar populations.

Figure 3 of Muñoz et al. (2013) shows the Color-Magnitude Diagram (CMD) of NGC 3201 with their data set and those of Carretta et al. (2009) and Simmerer et al. (2013). The Gonzalez & Wallerstein (1998) data set is shown in Figure 2 of their paper.

4. Discussion

We find that the data on iron abundance in the RGs of NGC 3201, analyzed in our original study (Kravtsov 2013) and in the present work, show increasing iron abundance with increasing radial distance from the cluster center, irrespective of both the facility used to gather observations and the methods of data reduction applied. All but one of the previous studies are based on observations gathered with fiber-fed multiobject spectrographs, except for five stars in the sample studied by Simmerer et al. (2013), which were separately observed with the MIKE spectrograph, presumably in standard slit observing mode. To our understanding, the only total set of spectra used by Gonzalez & Wallerstein (1998) to derive their data were obtained in standard slit observing mode. Therefore, it is of low probability that the trend of the same sense (iron abundance decreasing toward the center of NGC 3201) is reproduced with different data by chance.

The decrease in iron abundance toward the core of NGC 3201 might be real. If real, the primordial (first-generation) population of the GC should be concentrated in the core of NGC 3201, as found by Larsen et al. (2015) in the GC M15. In the case of NGC 3201, however, such a possibility seems to be improbable, because there is indirect evidence that the nitrogen-enriched population of RGB stars tends to be more concentrated toward the center of the cluster. This is implied by the result of Carretta et al. (2010), who coupled Na (and O) abundances for a limited sample of the cluster RGB stars with multicolor photometry available for a much larger number of RGB stars (Kravtsov et al. 2009), for which Kravtsov et al. (2010) showed a correlation between *U*-based photometric characteristics and radial distance from the cluster center. In

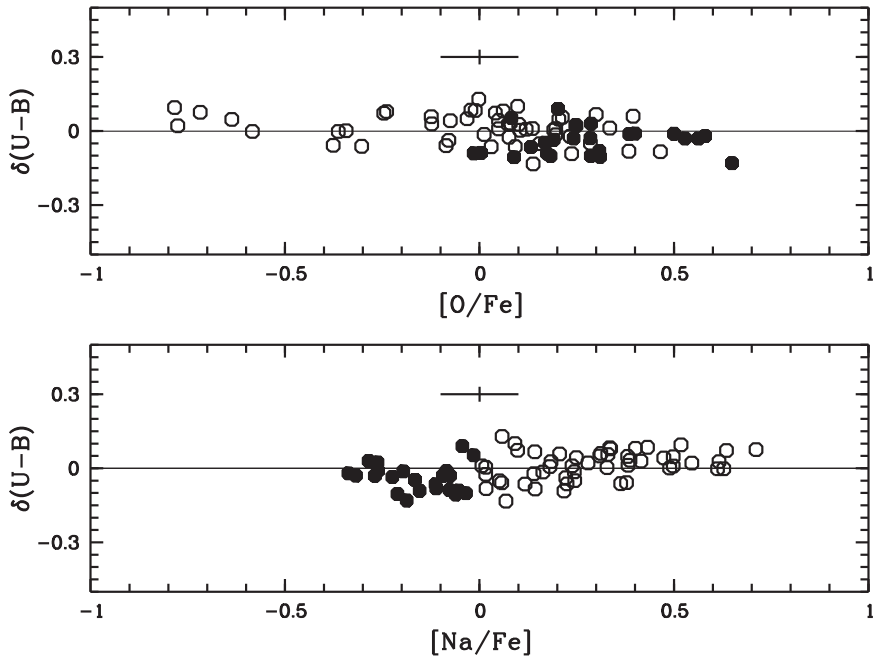

Figure 4. Dependence of the $(U - B)$ color of RGB stars, expressed as their deviations $\delta(U - B)$ from the RGB ridgeline in the dereddened $U - (U - B)$ diagram (Kravtsov et al. 2010), on the O and Na abundances (upper and lower panels, respectively) derived by Carretta et al. (2009) for the same stars. Filled circles show RGs defined by the latter authors as first-generation stars in NGC 3201, i.e., with [Na/Fe] < 0. The horizontal and vertical error bars show typical uncertainties in the abundance estimates and $(U - B)$ color, respectively. The latter is formally that of the photometry, and it does not include the uncertainty in dereddening corrections applied.

Figure 4, we summarize the relationship between the sodium and oxygen abundances derived by Carretta et al. (2009) for RGB stars in NGC 3201 and their abovementioned photometric characteristics as the dependence of the deviations $\delta(U - B)$ of these RGs from the ridgeline of the RGB, obtained by Kravtsov et al. (2010) from the cluster $U - (U - B)$ diagram corrected for differential reddening (see the referenced paper for more details). We show the RGB stars (filled circles) defined by Carretta et al. (2009) as first-generation stars. An additional point concerning this dependence is that the deviation $\delta(U - B)$ of RGs at a given abundance (of either sodium or oxygen) is, on average, larger at larger PRAD from the cluster center. This supplementary relation increases the width of the dependence along the $\delta(U - B)$ axis and makes it larger than the typical uncertainty of the photometry. In other words, at a given $\delta(U - B)$, RGs with higher oxygen (lower nitrogen) abundance are, on average, at a larger PRAD from the cluster center. Iron abundance does not show any detectable systematic variation between the extreme values of $\delta(U - B)$. The mean [Fe/H] value is within the error of the mean at any $\delta(U - B)$.

Although of low probability, a somewhat decreased iron abundance in the central part of NGC 3201 might be due to presently unknown detail(s) of star formation in GCs and subsequent dynamical evolution of the hosts. Our knowledge about the formation of massive (globular) star clusters is poor so far. There is a permanent inflow of new, sometimes challenging data on (radially depending relationship between) the kinematical and chemical characteristics of stellar populations in GCs. In particular, for a sample of the turnoff stars of 47 Tuc, Kucinskas et al. (2014) found the radial dependence of oxygen abundance and, moreover, a significant correlation between this abundance and the velocity dispersion of the stars. Also, Fabricius et al. (2014) found evidence of surprisingly ubiquitous central rotation (and its tight correlation with the central velocity dispersion) in a sample of 11 GCs, which can be assumed to be related to kinematically decoupled different stellar populations in the GCs.

It is obvious that the spectroscopic data is for the brighter RGs, with luminosity exceeding that of the RGB bump. The only exception is the sample of RGs studied by Carretta et al. (2009), which includes a large number of stars below the RGB bump. In general, there is no guarantee that the data on elemental abundances in brighter RGs will agree with those in lower RGs and particularly in main-sequence stars (e.g., Gratton et al. 2000, and references therein).

One could suppose that a systematic error originated from photometric factors due to erroneous corrections applied for differential reddening. A systematic effect might arise from the same type of multiobject fiber-fed spectroscopy used to gather the bulk of the observations. The sample of stars located at different radial distances from the cluster center might be affected by a systematically increasing sky background toward the center. The crucial condition for the varying sky background to affect the estimates of iron abundance in the central part of a GC seems to be a radially varying spectral composition of the background (i.e., varying its color) rather than increasing intensity at a constant color. Any notable color gradient of the background light, an important contributor to the light of any GC, should result in the radial color variations of the GC itself. In the last three decades, such variations were found in GCs, in the sense that the clusters were judged to be bluer, in addition to the strengthening of Balmer absorption lines, toward the centers of the GCs. This effect was discussed in a review of the topic by Djorgovski & Piotto (1993, and references therein). It is worth mentioning that most of these GCs are post–core-collapse objects, and the gradient typically extends to at least a few tenths of an arcsecond in radius and even up to $\sim 100''$ or further. "The typical $(B - I)$ gradient

amplitudes are ∼0.1–0.3 mag per decade in radius," according to estimates by Djorgovski et al. (1991). The weakest point of this argument is that it is unknown whether NGC 3201, which is irregularly reddened across its face, has a color gradient toward its center. This cluster is not a post–core-collapse system. The reality of the gradient of dereddened color is subject to dispute. An additional problem is to quantify the effect (if any) of the color gradient on iron abundance estimates deduced from a multiobject fiber-fed spectroscopy.

One might suggest a radial trend of the mass of coeval RGB stars at the same evolutionary stage as another alternative for mimicking the iron abundance trend in NGC 3201. Such a possibility seems to be not as exotic as it could be at first glance. On the contrary, the opposite assumption of no mass variation would be rather improbable, given the observational evidence of significant variation of the abundance of key chemical elements in stars of several GCs. In particular, nitrogen abundance, [N/Fe], is known to span about two orders of magnitude in RGB stars in NGC 6752 (Yong et al. 2008). In a general case, such large abundance variations in a GC, even being significantly compensated by the anticorrelated abundances of other main contributors (i.e., oxygen) to overall metallicity, can result in overall metallicity variations (at a constant iron abundance) of the order of a few tenths of a dex in the GC stars. The present-day GC stars of the same age but varying metallicity might have different masses. In the case of initial radial segregation of stars of different metallicity in a GC, one might expect that more centrally concentrated metal-rich stars would conserve their preferable central location in the GC during a Hubble time, due to their increased mass as compared to counterparts of lower metallicity. How could the mass difference be due to varying overall metallicity at a given constant iron abundance? We estimated it for this simplest case by computing two evolutionary tracks (Valcarce et al. 2012) using two models of the same iron and helium abundances, [Fe/H] $= -1.40$ and $Y = 0.250$, but of different mass and overall metallicity that allows the two tracks to achieve the end of RGB evolution at the same age. In more detail: (1) we imposed the values of the initial mass, M_1, and the overall metallicity, Z_1, for one model and computed the evolutionary track between the zero-age main sequence and the RGB tip, as well as the duration of the track; (2) then we imposed a higher metallicity, Z_2 ($Z_1 + \Delta Z$), and through iterative computations of models with this metallicity and varying mass, we searched M_2 such that its combination with Z_2 resulted in an evolutionary track with the same total lifetime as that of the track computed for the combination of Z_1 with M_1. By this method, the effect of varying metallicity on age was compensated by varying mass at the same iron abundance, [Fe/H] $= -1.40$, corresponding to NGC 3201. We finally estimated M_2 corresponding to the following combinations of varying mass with a plausible variation of metallicity in NGC 3201: $M_1 = 0.80 M_\odot$; $Z_1 = 0.00069$ ([O/Fe]$_1 = 0.0$) and $M_2 = 0.81\, M_\odot$; $Z_2 = 0.00115$ ([O/Fe]$_2 = 0.3$). We note that this does not mean that [O/Fe] should just be higher at higher Z. Instead, a higher [N/Fe] would be more natural. However, unfortunately, there was only the possibility of varying Z at the same [Fe/H] in the models computed. We used two available options for oxygen abundance, differing by 0.30 dex. This makes the mass difference as large as $\Delta M = 0.01\, M_\odot$. This is too small for a radial segregation of stars due to the dynamical evolution of a GC with no initial radial mass segregation (see more details in Larsen et al. 2015). For this mass difference and at the metallicity of NGC 3201, the temperature difference between the tracks ($\Delta T_{\rm eff} \approx 40$ K corresponding to $\Delta(B-V) \approx 0.03$ mag), in particular at the level of the RGB bump or above it, is comparable (in modulus) with the value necessary to result in the error of iron abundance of order Δ[Fe/H] $\sim$ 0.05 dex. Note that, according to Nataf et al. (2011), the same difference in [Fe/H] corresponds to $\Delta T_{\rm eff} \approx 17$ K at the metallicity of 47 Tuc (i.e., [Fe/H] $= -0.75$). The more important point is that in the framework of this simplified scenario for the considered models, they predict a radial dependence of photometric effects, some of which are in apparent disagreement with the observed ones. Specifically, the models predict decreasing brightness of the RGB bump toward the cluster center by magnitude depending on the photometric passband. In particular, the variation of the bump level is expected to be around $\Delta V \approx 0.18$ mag and to be larger and slightly smaller in U and I, respectively (Figure 5). The expected dependencies of the RGB bump magnitude on both radial distance from the cluster center and used passband are in disagreement with the apparent behavior of the bump level in NGC 3201 as implied by cluster photometry obtained by Kravtsov et al. (2009).

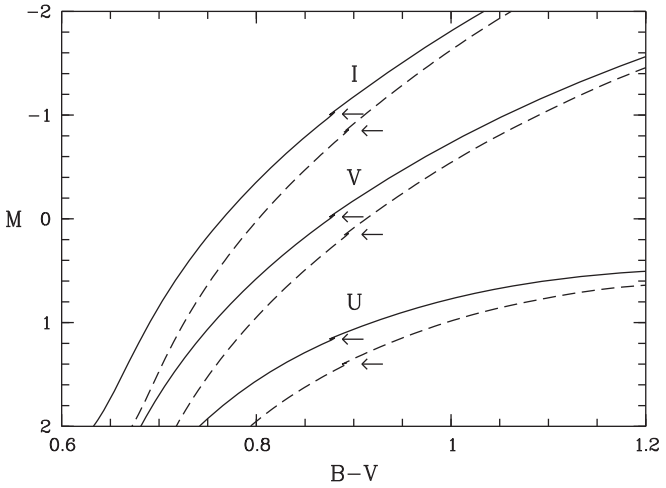

Figure 5. Two evolutionary tracks (Valcarce et al. 2012) are shown in the CMD with the $(B-V)$ color and different absolute magnitudes in the I, V, and U passbands. The solid and dashed lines are the tracks computed for the same age and iron and helium abundance, [Fe/H] $= -1.40$ and $Y = 0.250$, but for different mass and overall metallicity, $M_1 = 0.80\, M_\odot$; $Z_1 = 0.00069$ ([O/Fe] $= 0.0$) and $M_2 = 0.81\, M_\odot$; $Z_2 = 0.00115$ ([O/Fe] $= 0.3$), respectively. The arrows indicate the predicted position of the peculiarity in the models' RGB evolution, which is responsible for the occurrence of the RGB bump.

No significant radial trends are normally expected in GCs, given their typical relaxation time. In general, therefore, a radial variation of the RGB bump level (in the V magnitude) in a typical GC is expected to be none or negligible, i.e., within the threshold of its real detectability. In any case, reliable detection of such a variation of the RGB bump brightness of the order of $\Delta V \sim 0.05$ mag is a challenging task. It can have credibility provided that, besides known requirements imposed on both the accuracy of photometry and the sample size of RGs belonging to the RGB bump, there must be insignificant uncertainty in the reddening variation across the cluster face, within $\delta E(B-V) < 0.005$ mag, so that the uncertainty in extinction variation would not be more than the typical rms of photometry, $\delta A_{\rm v} \sim \sigma \sim 0.010$–$0.015$ mag. Unfortunately, NGC 3201 does not meet this condition, since its reddening

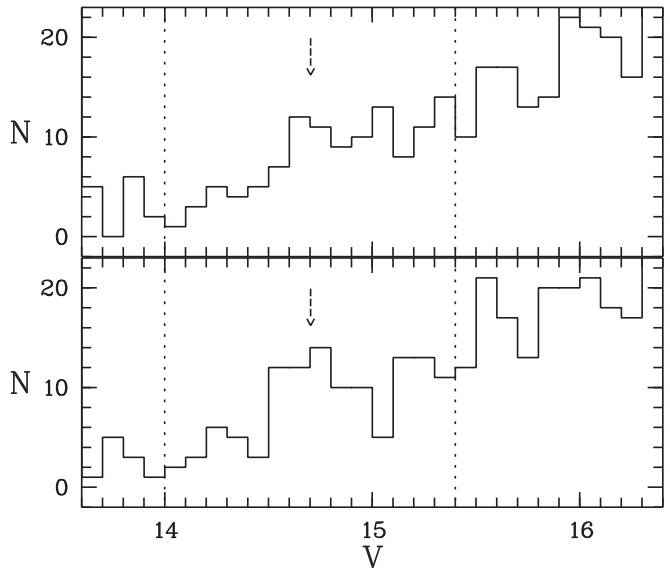

Figure 6. Part of the RGB LF obtained by Kravtsov et al. (2009) in the V magnitude corrected (top panel) and uncorrected (bottom panel) for differential reddening in NGC 3201. The arrows mark the position of the RGB bump, while the dotted lines show the voluntarily imposed range of the bump region. The dependence of the LFs in both the V and U magnitudes on PRAD from the cluster center is demonstrated in Figure 7.

is highly and irregularly variable (e.g., von Braun & Mateo 2001). Any reddening-corrected photometry would have ± 0.05 mag measurements with residual errors in reddening correction of the order of $\delta E(B-V) \sim \pm 0.015$, i.e., 3–4 times as large as the abovementioned limiting value. This is converted in residual magnitude error $\delta V \sim \pm 0.05$ mag due to the uncertainty in reddening correction. This can make it hardly possible to reliably establish and quantify RGB bump variation within $\Delta V < 0.10$ mag in NGC 3201 as was observed in 47 Tuc (Nataf et al. 2011), especially taking into account a notably smaller number of RGs in the former GC.

To draw any conclusion about this subject, we examined the radial behavior of the RGB bump luminosity function (LF) in three passbands. In V and U, we used photometric data corrected and uncorrected for differential reddening and uncorrected in I. To achieve this goal, we relied on multicolor photometry made by Kravtsov et al. (2009) in a fairly large cluster field. In particular, we used the same data sample on RGs that were selected and decontaminated by the authors in their original analysis of the cluster RGB LF (note, however, that the same result is achieved without any decontamination). Thus, we refer readers to that paper for more details relevant to the subject. Figure 6 shows a fragment of RGB LFs in the V magnitude corrected (top panel) and uncorrected (bottom panel) for differential reddening in NGC 3201. The arrows mark the resulting apparent position of the RGB bump in the LFs for the total sample of RGs, whereas the dotted lines show the $V(V_c)$ magnitude range of $\Delta V(V_c) = 1.4$ mag tentatively defined as the RGB bump region, i.e., within ± 0.70 mag around the RGB bump position.

As seen in Figure 6, we scan a broad RGB bump region to show the structure of the bump, while noting that the number of RGs in this region is limited. The latter factor did not allow us to reliably estimate the position of the bump at different PRAD from the cluster center. Thus, our main goal was to examine whether there is a tendency in the radial variation of the bump level and to make rough quantitative estimates. The LFs in U and U_c (and in I) were obtained by simply using the respective magnitudes of the RGs selected by their V and V_c magnitudes. In other words, the LFs of the RGB bump region in U and U_c (and in I) are exactly the same as the RGs that were selected by their V and V_c magnitudes. In Figure 7, we show the dependence of the LF of the RGB bump region on PRAD from the cluster center. These LFs are for three overlapping cluster areas with increasing (top to bottom panels) mean PRAD from the cluster center. The number of RGs falling into the specified bump range is virtually the same in each area. Since the photometry used was made in a square area ($14' \times 14'$) centered on the cluster, the external border of the outer region is not circular, and the longest PRAD of stars in this region, $R_{\max} \approx 10'$, is achieved in the corners of the area. To increase the reliability of our analysis, we excluded the central cluster, within PRAD $R < 42''$ (100 pixels), from our consideration, thereby at least reducing potential problems that might be caused by a systematic error due to crowding effects and possible somewhat different completeness at a fainter and brighter magnitude of the bump just in the central cluster region. The photometry by Kravtsov et al. (2009) was shown to be in very good agreement with that by Stetson (2000) in V, I. The agreement with photometry by Layden & Sarajedini (2003) was also very good in the V passband but somewhat poorer in the I passband due to a systematic difference between the two data sets that was magnitude-dependent.

The LFs in the V magnitude show a tendency of displacement of the RGB bump level toward fainter magnitudes in the outer part of NGC 3201; we detect an apparently decreasing proportion between the number of RGs at $V \leqslant 14.70$ and that at fainter magnitudes. One can note also that (1) this tendency is the same, in principle, in both the V and V_c magnitudes and (2) notable transformations in the LFs begin to occur somewhere in the range of PRAD $2' < R < 3'$. In the central part of the cluster, the bump is surely detected and confidently fixed at $V \approx 14.70$. Estimating the exact position of the bump in the outer part, at $R > 175''$, is unreliable. The displacement of the bump toward fainter magnitudes may be as large as $\Delta V \sim 0.15$ mag. Here, we have to stress that this variation cannot be explained by a spurious brightening of RGB stars toward the center of NGC 3201 due to a systematic effect of the photometry in the crowded central region. This possibility is in fact ruled out, since Nataf et al. (2013) found the bump location at $V = 14.649 \pm 0.032$ by relying on *HST* photometry of the (central part of the) GC NGC 3201. This bump location is in very good agreement with and virtually indistinguishable from that seen in the left upper panel of Figure 7. The LFs in the V_c magnitude show virtually the same radial variation of the bump position. Relying on these LFs, the displacement can be estimated as being as large as $\Delta V_c \sim 0.20$ mag. Separately, the left panels of Figure 8 show the dependence of the RGB bump region LF in the I passband on PRAD from the cluster center. For comparison, the same dependence relying on photometry made in the cluster by Layden & Sarajedini (2003) is presented in the right panels. The sample stars are those in common in the two data sets. One can note that (1) the radial behavior of the RGB bump LF in the I and $V_c(V)$ (Figure 7) passbands is very similar, and (2) the LFs obtained from the two data sets show virtually indistinguishable radial dependence in spite of some disagreement between photometries by Layden & Sarajedini (2003) and Kravtsov et al. (2009) in the I passband.

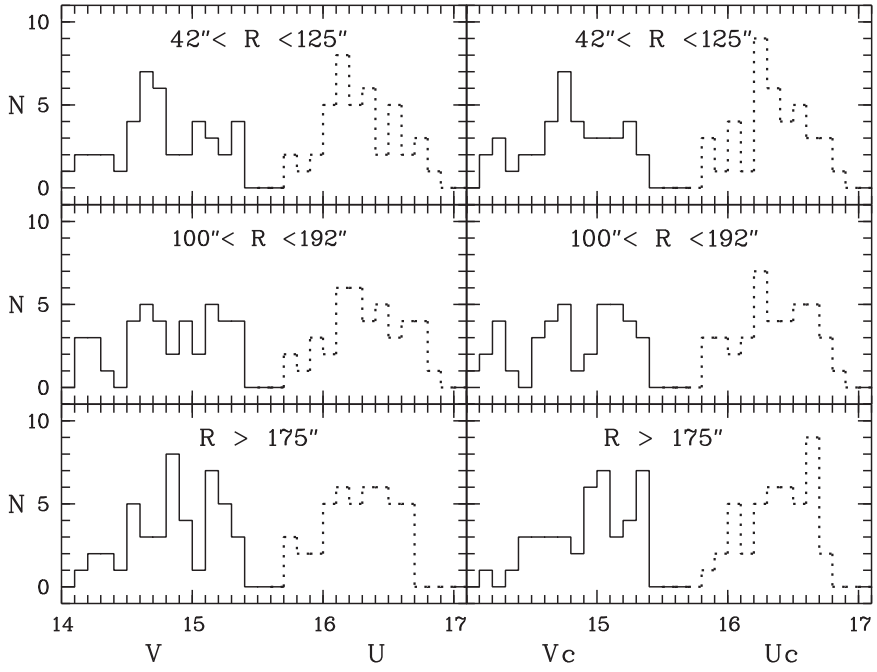

Figure 7. Dependence of the LF of the RG bump region, defined as shown in Figure 6, in the V (solid lines) and U (dotted lines) passbands on PRAD from the cluster center in a $14' \times 14'$ cluster field. Left and right columns show the LFs based on red giant magnitudes uncorrected (V; U) and corrected (V_c; U_c) for differential reddening (Kravtsov et al. 2009), respectively. In each column, the panels (top to bottom) show the LFs for three consecutive cluster regions with increasing PRAD from the cluster center. Indicated in the panels are the ranges of the PRAD, R (expressed in arcseconds), limiting each region. The upper limit of the PRAD of RGs in the outermost region is $R_{\max} \approx 10'$.

Kravtsov et al. (2009) estimated differential reddening in the observed field of NGC 3201 from shifts of the CMDs, relative to each other, of elemental areas composing the field "provided reddening is what is fully responsible for these shifts." However, it is now known that there are probable additional photometric effects caused by "multiple stellar populations" in the cluster CMDs, which are normally more pronounced in both the U passband and U-based colors due to CNO molecular bands located in the UV part of the spectrum. Also, interstellar extinction is stronger at shorter wavelengths. Therefore, a variable reddening would result in a larger scatter in the U magnitudes of stars than in the B, V, and especially I magnitudes. Thus, the effects caused by the two factors are entangled, and the U magnitude seems to be the most affected. Interesting enough, it is in the U magnitude that the LFs of the bump region show very small or even no radial variation.

To quantify and check the noted apparent radial behavior of the bump, we calculated and used the mean magnitudes ($\overline{U}$, $\overline{U_c}$, $\overline{V}$, $\overline{V_c}$, and $\overline{I}$) of the isolated bump region in the respective cluster regions and passbands. Strictly speaking, such an estimate is not fully equivalent to the direct estimate of the bump position, but the former seems to be more conservative than the latter. The mean magnitudes and respective rms values (σ) were calculated using the relevant command of the MIDAS system. We also calculated the uncertainties in the means (σ_m), taking into account the number of stars falling in the defined magnitude range (n and n_c for the magnitudes uncorrected and corrected for differential reddening, respectively) of the bump region in each of the three cluster regions considered. The obtained data are listed in Table 1. They support the apparent behavior of the RGB bump LFs at a different radial distance from the cluster center and show that the difference between the mean magnitudes of the bump region in the outer and inner cluster fields increases with increasing wavelength. For the uncorrected mean magnitudes, in particular, it changes from being obviously smaller than the error of the difference between the means in the U passband and up to $\Delta\overline{I} = 0.13$ mag, a factor of 1.5 as large as the respective error in the I passband. We carried out the same study and made the same estimates for the GC NGC 6752 using multicolor cluster photometry by Kravtsov et al. (2014). The photometric data for both GCs were obtained using observations gathered with the same facility. The radial variation of the mean magnitude of the bump region (and the bump itself) in NGC 6752 depends on wavelength in the opposite sense as for NGC 3201: it is insignificant or none in I and the largest in U. Kravtsov et al. (2014) pointed to and showed a notable radial variation of the RGB bump level in the U magnitude in the sense that it is brighter in the outer part of NGC 6752. Therefore, the dependence of the bump level on radial distance in these GCs is in the opposite sense as well.

Note that photometric effects in the U passband may turn out to be dissimilar in different data sets in the same GC depending on the exact response curve of the U passband. Specifically, the response curve of the standard U passband of the UBV photometric system should, by definition, encompass the Balmer jump. For RGs observed from different facilities, it may be difficult to directly compare U measurements because the strong CNO features may cause nonnegligible photometric effects. This is caused by the passband modified so that the maxima of their response curves are approximately 150–200 Å or even more blueshifted to exclude the Balmer jump, as described in Kravtsov et al. (2007, and references therein). The response curve of the U passband used for photometry of NGC 3201 by Kravtsov et al. (2009) is close to the standard U passband, and it is shown in Kravtsov et al. (2014).

The tendency (we stress that one can only refer to a tendency) in both the apparent behavior of the RGB bump LFs

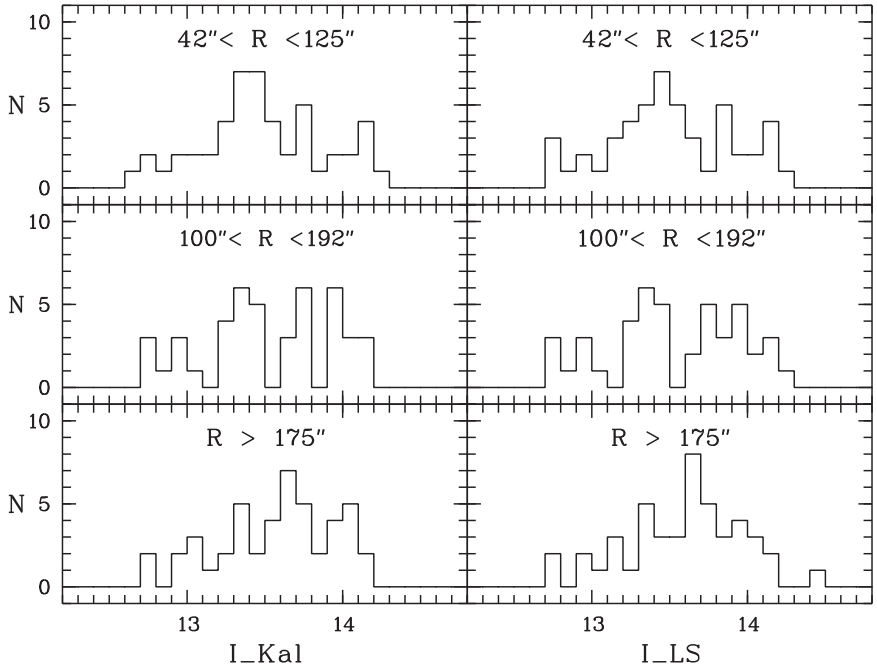

Figure 8. Comparison of dependence of the RG bump region LF, defined as shown in Figure 6, in the *I* passband on PRAD from the cluster center. The left and right panels show the dependence based on the photometry of Kravtsov et al. (2009) and Layden & Sarajedini (2003), $I_{\rm Kal}$ and $I_{\rm LS}$, respectively. The uncertainty in the number of stars, *N*, falling in each bin in all the histograms showing RGB bump LFs (including Figure 7) is $\pm\sqrt{N}$.

in different passbands and the estimates quantifying this behavior disagrees with the scenario that suggests overall metallicity as a unique radially varying parameter increasing toward the cluster center. We stress again the point that the variation in the overall metallicity at a constant [Fe/H] ratio was achieved by varying the [O/Fe] ratio. It is unclear how the bump level will depend on overall metallicity in case of variations in nitrogen or carbon abundances only or of any combination of the CNO components. This tendency would agree somewhat better (in *V* and *I* but not in *U*) with decreasing metallicity toward the cluster center. However, the magnitude of the decreasing [Fe/H] ratio toward smaller *R* (within PRAD $R \approx 9'$) is insufficient to cause a detectable variation of the bump level, since this variation would be within the extinction uncertainty. For this reason, we examined another important contributor to the overall metallicity that could be responsible for the radial variation of the bump level.

Having analyzed the data of Carretta et al. (2009) on oxygen and sodium abundances in NGC 3201, we found a radial trend of the [O/Fe] ratio in the same sense as the radial trend of iron abundance, i.e., decreasing oxygen abundance toward the cluster center. The upper left panel of Figure 9 shows the trend in the $R-$[O/Fe] diagram. In turn, the lower left panel demonstrates an obvious correlation between oxygen and iron abundances in RGs of NGC 3201. As seen in Figure 9 and estimated from the data, the oxygen abundance variation can be as large as Δ[O/Fe] ~ 0.3 dex within PRAD $R \approx 9'$. We computed and analyzed stellar models that mimic the same change in the [O/Fe] ratio we detected in NGC 3201; we found that the models predicted a comparable bump-level variation in the *V*- and *I*-band simulated data (Figure 5). Also, both the predicted and suspected radial dependencies of the bump level are of the same sense: the bump magnitude is fainter at a higher [O/Fe] ratio, i.e., at larger PRAD from the cluster center. According to the same models, the variation of the bump level would be larger in the *U* passband and smaller in the *I* passband, contrary to the observed dependence in NGC 3201. It should be noted in this context that the two models we rely on are different only by oxygen abundance, and the abundances of other key elements, in particular carbon and nitrogen, remain (nearly) unchangeable. As for the real situation in NGC 3201, there is no guarantee that the radial trend of oxygen (and iron) abundance is not accompanied by a trend of C and/or N abundances. Indeed, Figure 9 shows that there is a radial variation of the [Na/Fe] ratio of a smaller amplitude and in the sense opposite to that of both the [O/Fe] and [Fe/H] ratios. Since sodium and nitrogen abundances are known to correlate with each other in RGs, the radial trend of the former implies a same-sign trend of the latter (i.e., of nitrogen abundance) in the cluster. An interesting relationship can be noted here: the data of Carretta et al. (2009) do not reveal any radial trend of both the [O/Fe] and [Na/Fe] ratios in NGC 6752, where radial variation of the RGB bump level, as was noted above, is also dissimilar to that in NGC 3201.

A problematic point should be mentioned. There is a lack of agreement between the RGB bump level variation at different PRAD from the cluster center, on the one hand, and the appearance of some features of the CMDs (with different colors and magnitudes) in the same parts of the cluster, on the other. For example, a fainter bump level (in *V* and *I*) in the outer than in the inner part of the cluster is in agreement with higher oxygen and iron abundances (but presumably lower nitrogen and carbon abundances) in the former than in the latter, but the shape of the turnoff region and the slope of the subgiant branch in the CMDs of the outer cluster part apparently correspond more to a more metal-poor population than the central part. We do not know anything about the radial behavior of carbon abundance and the overall metallicity in NGC 3201. Hence, a somewhat higher overall metallicity in the central part of NGC 3201, or at least no radial variation of the overall metallicity, cannot be ruled out.

Table 1
Mean Magnitudes of the RGB Bump Region at Different Radial Distances

Area[a]	n; n_c	$\overline{U}$	σ_m	σ	$\overline{U_c}$	σ_m	σ	$\overline{V}$	σ_m	σ	$\overline{V_c}$	σ_m	σ	$\overline{I}$	σ_m	σ
inn	42; 40	16.29	0.04	0.28	16.34	0.04	0.25	14.77	0.06	0.36	14.79	0.05	0.34	13.50	0.06	0.39
int	41; 40	16.34	0.05	0.29	16.35	0.05	0.28	14.82	0.06	0.38	14.81	0.06	0.38	13.55	0.06	0.40
out	45; 43	16.27	0.04	0.26	16.37	0.04	0.24	14.87	0.05	0.34	14.94	0.05	0.33	13.63	0.06	0.37

Note.
[a] The "inn," "int," and "out" areas denote those cluster regions, radially getting away from the cluster center, the RGB bump LFs of which are shown in the upper, middle, and lower panels of Figure 7, respectively.

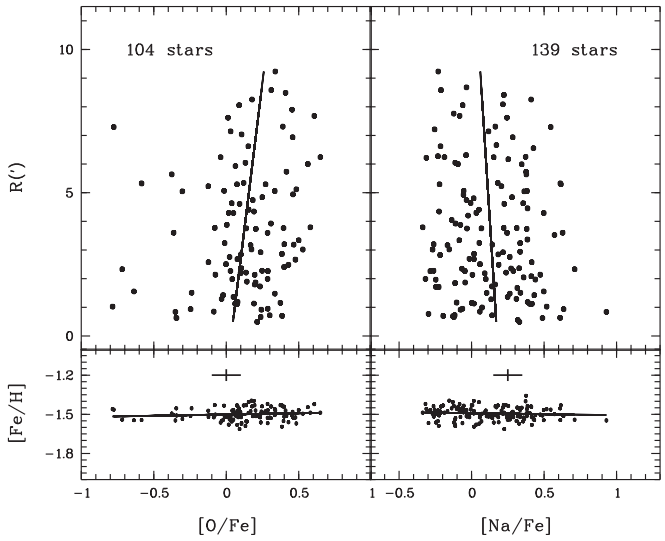

Figure 9. The upper left and right panels show the dependence of oxygen and sodium abundances in 104 and 139 RGs, respectively, on the stars' PRAD from the center of NGC 3201, as inferred from the data of Carretta et al. (2009). The lower panels show the relationship between these abundances and that of iron in the same stars. The solid lines are linear fits to the data.

The real situation within NGC 3201 may be more complicated than the presence of radially varying abundances of the key elements. A promising parameter to play a role is the radially increasing rotational velocity of stars in the GC, which "allows" the stars to be somewhat more massive at the same age (and even more at younger ages) than the more slowly rotating (and older) counterparts. Comparison of models with and without rotation (Georgy et al. 2013) shows that the upper limit of mass difference between the present-day RGB stars in a GC with overall metallicity $Z = 0.002$ could be as large as $\Delta M \sim 0.05 M_\odot$ under an assumption that rotating models (initial equatorial velocity on the zero-age main sequence is $\sim$10 km s^{-1} for the initial mass around $M_{\rm in} = 0.80\,M_\odot$) are of younger age, within 1 Gyr, and the same helium abundance. Increasing helium abundance in rotating RGB stars should decrease ΔM. The effect of slightly increased ΔY (by $\sim$0.01–0.02) on ΔM can be compensated by a somewhat higher ($\sim$0.15 dex) overall metallicity. We thus conclude that the largest value of ΔM, even somewhat larger than 0.05 $M_\odot$, can formally be achieved in a GC if rotating RGB stars are more metal-rich and younger but have the same helium abundance as their nonrotating counterparts. Assuming the existence of two distinct subpopulations in NGC 3201, Wagner-Kaiser et al. (2016) estimated (the upper limit of) the helium difference among them at around $\Delta Y = 0.06$. If real, such a fairly large difference in helium abundance would rule out the possibility of increased mass of the centrally located subpopulation of stars in the cluster. At this point, two comments should be made. First, the lowest metallicity ($Z = 0.002$) of the available rotating models is higher than the metallicity of NGC 3201, and, strictly speaking, ΔM may be smaller at lower metallicity. By contrast, the real difference (if any) between the typical initial rotational velocities of the stars (of a given initial mass) of the two assumed subpopulations is an unknown quantity, and it could be higher than the unique option available for the rotating models. Moreover, we do not have reliable information about the real (radial) variation of the overall metallicity in NGC 3201. Second, the rotating models do not, unfortunately, fully trace the RGB but only its lower part and do not even achieve the level of the RGB bump. These limitations impose serious constraints on or exclude a more complete analysis.

A higher-metallicity RG can have a higher mass than a comparable star of lower metallicity. In turn, both a faster rotation and a higher mass make the RGB and its bump brighter (and hotter), partially compensating for the opposite effect of increasing metallicity (if any) on the temperature and luminosity toward the cluster center or making the bump brighter at a constant metallicity. On the other hand, the same-sign radial trends of the mass and rotational velocity will result in opposite-sign (compensating each other) effects on the rate of stellar evolution, thereby allowing an RGB star to be more massive than its more metal-poor and slowly rotating counterparts at the same point in their evolution. Unfortunately, the available models with rotation do not allow a study of this subject in more detail to estimate the variation of both the luminosity and temperature of the RGB bump as a function of metallicity and rotational velocity. However, we refer to Brown & Salaris (2007), who estimated quantitatively (for a given set of age, metallicity, etc.) the impact of rotation on increasing brightness of the RGB bump. It should be stressed that the combined effect of the parameters under consideration on the RGB stars and on the bump level must be in agreement with the respective effect of the same parameters on the horizontal-branch stars. It is pertinent to note in the context of our present study that Tailo et al. (2015) arrived at the conclusion of rapidly rotating second-generation stars in the GC ω Cen.

Considering the variation of the He abundance at the same age and range of rotational velocity of GC stars, ΔM should be lower or even zero, depending on ΔY. The possibility of a detectable mass difference among RGB stars in GCs with a (large) variation of the N abundance is implied by a very recent result on the field RGB stars: Martig et al. (2016) found a tight correlation between the mass of RGB stars and the ratio of their N and C abundances at a given [Fe/H], $T_{\rm eff}$, and log g. In the context of GC multiple populations, is there any variation in the N/C ratio at a given $T_{\rm eff}$ and log g among RGB stars within separate monometallic GCs? There is a need for further study

of possible mass, rotational velocity, and *N/C* ratio variations among RGB stars in GCs (see Gratton et al. 2012).

Note that increasing mass and/or rotational velocity and/or helium abundance of stars toward the GC centers are in agreement with colors getting bluer toward the same direction.

To complete the discussion, we summarize the results derived from the older data sets as follows. (1) Hα emission is present in the spectra of four sample stars of Gonzalez & Wallerstein (1998). (2) The mean [Fe/H] value of these RGs is somewhat lower than that for the rest of the stars. (3) The most metal-poor sample star, Côté 246, shows the strongest Hα emission.

5. Conclusions

We studied the unusual radial trend of the iron abundance in the GC NGC 3201. It was originally found, at a statistically significant level in some GCs including NGC 3201, as a slightly decreasing [Fe/H] ratio in RGs toward the GC centers by relying on the data of Carretta et al. (2009) alone.

We discovered that the trend is reproduced by distinct data on iron abundance independently derived for the same GC. We compared four sets of data obtained by different authors using observations gathered with different facilities and/or reduced independently, but all the data are dominated by those of Carretta et al. (2009) until more can be gathered for distant RGB stars.

The data of Simmerer et al. (2013), based on FLAMES-UVES and MIKE spectra, also reveal a trend of the same sense (more centrally concentrated LIA RGs) at a marginally statistically significant level. Mucciarelli et al. (2015) reanalyzed the same FLAMES-UVES spectra and reported on a negligible spread of iron abundance derived from Fe II spectral lines. We find that these data support the trend at a high confidence level of 92%. The trend is virtually indistinguishable, within the error, from that originally found using the much larger sample size of Carretta et al. (2009)'s data. Additionally, we notice that both data sets are indistinguishable from each other with respect to their standard deviations giving evidence of the same scatter in the data. Revising the present paper, we additionally considered the data of Gonzalez & Wallerstein (1998) on iron abundance derived for 18 RGs. Although this sample size is smaller than those of other considered data sets, five sample stars were observed and studied at an unprecedentedly longer radial distance from the cluster center than ever reached in other studies in NGC 3201. Interestingly enough, these RGs are obviously more iron-rich than the rest of the stars, thereby supporting (at least formally) the presence of the trend under consideration. According to Gonzalez & Wallerstein (1998), an effect of a systematic error cannot be excluded, though. Apart from the apparent trend in [Fe/H], we found evidence for a more pronounced trend in oxygen abundance toward the cluster center. The variation of the [O/Fe] ratio in RGs as a function of radial distance from the cluster center can be as large as Δ[O/Fe] $\sim$ 0.3 dex within PRAD $R \approx 9'$.

We considered and discussed a number of causes and effects that might mimic the radial variation of iron abundance. The same effects could, however, hardly mimic the notable trend of oxygen abundance as well, taking into account the presence of a similar radial trend of the [Fe/H] ratio in the GC NGC 6752 but no apparent oxygen abundance trend. These effects might be related to the physical characteristics of the studied objects themselves, in particular, to a faster rotation and a higher mass of centrally located RGs. Both of these parameters should make RGs somewhat hotter and brighter than their less massive and more slowly rotating counterparts (at least at the same overall metallicity and helium abundance), but simultaneously they have opposite, mutually compensating effects on the timescale of stellar evolution. A younger age of rotating stars strengthens these effects. The RGB bump LFs show a tendency for the bump to became brighter toward the cluster center in the *V* and *I* (but presumably not *U*) passbands. However, the radial trend of the rotational velocity and mass of RGs in NGC 3201 could hardly be responsible for the estimated magnitude of the brightening of the bump level toward the cluster center. It could not be the main contributor to the brightening. Several radially dependent photometric effects can alter the appearance of CMDs with different magnitudes and colors that contradict each other and need to be reconciled. Partially, this can be caused by the combined effects of "multiple populations" and irregularly varying reddening. An increasing nitrogen abundance toward the cluster center is possible. Also, radially increasing carbon abundance in the same sense cannot be ruled out, since the abundances of these two elements are known to correlate with each other in GCs. Helium abundance slightly increasing (by $\Delta Y \sim 0.01$–0.02) toward the cluster center cannot be excluded either.

Stellar rotation is an important parameter poorly considered in present-day studies of GCs. An increased rotation of more centrally located RGs in GCs, especially in combination with their higher metallicity and younger age, could potentially lead to a nonnegligible radial variation of mass, increasing toward the cluster center, among RGs of the same evolutionary stage. Another alternative may be that NGC 3201 might have been of notably higher mass in the past, and the primordial radial effects in the initial GC might be partially conserved. Also, tidal stripping removes lower-mass stars first and concentrates higher-mass stars and binaries in the core. This GC is well known by its unusual kinematics in the Galaxy (Harris 1996), and the origin of NGC 3201 is not clear.

Finally, the analysis presented in our study shows that the bulk of the data on iron abundance in particular and elemental abundances in general in NGC 3201 was obtained for stars located within radial distance $R \approx 9'$. There is a lack of reliable information and therefore intriguing uncertainty about the radial dependence of iron (elemental) abundance(s) at (much) larger radial distances from the cluster center, since the measurements made by Gonzalez & Wallerstein (1998) for five stars in the range $13' < R < 26'$ from the cluster center are the unique data obtained in the outer(most) part of NGC 3201.

The author thanks the anonymous referee for useful comments and suggestions that improved the manuscript. This research has made use of the VizieR catalog access tool, CDS, Strasbourg, France.

ORCID

Valery V. Kravtsov https://orcid.org/0000-0002-9799-5889

References

Brown, D., & Salaris, M. 2007, in AIP Conf. Proc. 948, Unsolved Problems in Stellar Physics: A Conf. in Honor of Douglas Gough (Melville, NY: AIP), 315

Carretta, E., Bragaglia, A., D'Orazi, V., Lucatello, S., & Gratton, R. G. 2010, A&A, 519, 71
Carretta, E., Bragaglia, A., Gratton, R. G., et al. 2009, A&A, 505, 117
Carretta, E., Bragaglia, A., Gratton, R. G., Lucatello, S., & Momany, Y. 2007, A&A, 464, 927
Carretta, E., Lucatello, S., Gratton, R. G., Bragaglia, A., & D'Orazi, V. 2011, A&A, 533, 69
Côté, P., Welch, D. L., Fischer, P., et al. 1994, ApJS, 90, 83
Covey, K. R., Wallerstein, G., Gonzalez, G., & Vanture, A. D. 2003, PASP, 115, 819
Djorgovski, S., & Piotto, G. 1993, in ASP Conf. Ser. 50, Structure and Dynamics of Globular Clusters, ed. S. G. Djorgovski & G. Meylan (San Francisco, CA: ASP), 203
Djorgovski, S., Piotto, G., Phinney, E. S., & Chernoff, D. F. 1991, ApJL, 372, L41
Fabricius, M. H., Noyola, E., Rukdee, S., et al. 2014, ApJL, 787, L26
Georgy, C., Ekstrom, S., Eggenberger, P., et al. 2013, A&A, 558, 103
Gonzalez, G., & Wallerstein, G. 1998, AJ, 116, 765
Gratton, R. G., Carretta, E., & Bragaglia, A. 2012, A&ARv, 20, 50
Gratton, R. G., Sneden, C., Carretta, E., & Bragaglia, A. 2000, A&A, 354, 169
Harris, W. E. 1996, AJ, 112, 1487
Kravtsov, V. 2013, A&A, 554, L6
Kravtsov, V., Alcaíno, G., Marconi, G., & Alvarado, F. 2007, A&A, 469, 529
Kravtsov, V., Alcaíno, G., Marconi, G., & Alvarado, F. 2009, A&A, 497, 371
Kravtsov, V., Alcaíno, G., Marconi, G., & Alvarado, F. 2010, A&A, 512 L6
Kravtsov, V., Alcaíno, G., Marconi, G., & Alvarado, F. 2014, ApJ, 783, 56
Kucinskas, A., Dobrovolskas, V., & Bonifacio, P. 2014, A&A, 568, L4
Larsen, S. S., Baumgardt, H., Bastian, N., et al. 2015, ApJL, 804, 71L
Layden, A. C., & Sarajedini, A. 2003, AJ, 125, 208
Martig, M., Fouesneau, M., Rix, H.-W., et al. 2016, MNRAS, 456, 3655
Mucciarelli, A., Lapenna, E., Massari, D., Ferraro, F. R., & Lanzoni, B. 2015, ApJ, 801, 69
Muñoz, C., Geisler, D., & Villanova, S. 2013, MNRAS, 433, 2006
Nataf, D. M., Gould, A., Pinsonneault, M. H., & Stetson, P. B. 2011, ApJ, 736, 94
Nataf, D. M., Gould, A. P., Pinsonneault, M. H., & Udalski, A. 2013, ApJ, 766, 77
Simmerer, J., Ivans, I. I., Filler, D., et al. 2013, ApJL, 764, L7
Stetson, P. B. 2000, PASP, 112, 925
Tailo, M., DAntona1, F., Vesperini, E., et al. 2015, Natur, 523, 318
Valcarce, A. A. R., Catelan, M., & Sweigart, A. V. 2012, A&A, 547, 5
von Braun, K., & Mateo, M. 2001, AJ, 121, 1522
Wagner-Kaiser, R., Stenning, D. C., Sarajedini, A., et al. 2016, MNRAS, 463, 3768
Yong, D., Grundahl, F., Johnson, J. A., & Asplund, M. 2008, ApJ, 684, 1159